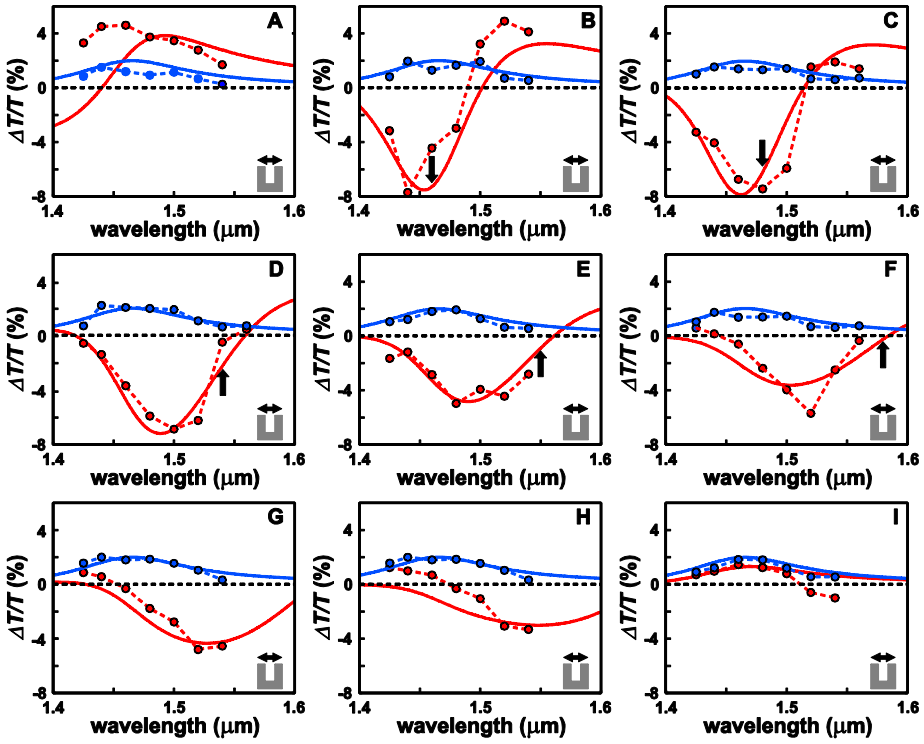

Fig. 4. Summary of femtosecond pump-probe experiments (like exemplified in Figs. 2 and 3) for various SRR arrays. The OPO probe polarization is horizontal. For reference, the measured linear optical spectra of the corresponding SRR arrays are shown in Fig. 1(d). The color coding is the same as in Figs. 2 and 3. Spectra of the differential transmittance signal are shown versus OPO probe wavelength for a fixed time delay of Δt = + 5 ps. Dots connected by dashed straight lines correspond to the experiment, the solid curves are derived from the toy model (parameters are given in the main text). The plasmonic resonance frequencies of the toy model quoted in Table 1 are illustrated by the black arrow in sub-panels B to F; for the other panels the resonances lie outside the wavelength range shown here.

The behavior of the magnitude of the differential transmittance signal in Fig. 2 is also consistent with this interpretation. For a QW with SRR, the modulus of the signals is a factor of about 5 larger than for the case of the bare QW. In Section 4, we will show that this measured behavior is consistent with the toy model, the physics of which has been explained in the introduction (Section 1).

We have taken complete data sets similar to that in Fig. 2 for several other SRR arrays. A second example is shown in Fig. 3. Here, the SRR resonance is largely blue-detuned with respect to the QW gain spectrum, resulting in an off-resonant situation. As expected on the basis of the qualitative discussion in our introduction, we observe a positive differential signal when probing the spectral wings of the SRR resonance. To give an overview on all these results, we compress the data as shown in Fig. 4. Here, we use the same color coding as in Figs. 2 and 3 and merely plot the differential transmittance signal at small positive time delay, *i.e.*, for Δt = + 5 ps, versus the OPO probe wavelength. It becomes obvious that negative $\Delta T/T$ signals for the case of QW and SRR are the rule rather than the exception. In contrast, the $\Delta T/T$ signals are always positive (and generally smaller in magnitude) for the bare QW. Close to resonance between the SRR resonance and the QW gain peak, the behavior is similar to that shown in Fig. 2. For more off-resonant SRR arrays, the differences between QW and SRR and QW alone become smaller – as expected from resonant coupling between the SRR resonance and the QW gain.

4. Comparison with toy model

To obtain a better understanding for the fairly complex measured behavior shown in Figs. 2-4, we compare these data with the above-mentioned toy model that has been defined in detail in [14]. We refer the reader to the mathematics therein. In Section 1 of the present paper, we have already revisited the underlying physics.

Clearly, this toy model [14] has quite a few free parameters: For the resonances of SRR and QW, respectively, one can choose the resonance position Ω, the damping γ, the number density N and the dipole matrix element d – four parameters each. In addition, the local-field coupling parameter L is purely heuristic. Altogether, this makes 9 adjustable parameters. However, the four parameters for the QW gain resonance can already be adjusted on the basis of the experiments on the bare QW (see Fig. 4) where the background dielectric constant is set to $(3.1)^2$. The number density of the SRR can be taken from Fig. 1(c), the other three parameters for the SRR resonance without gain (*i.e.*, without optical pumping) can already be adjusted according to the linear optical spectra of the SRR arrays. Note that the plasmon resonance frequencies referring to low sample temperature listed in Table 1 are consistently blue-shifted with respect to the minima in the room-temperature transmittance spectra shown in Fig. 1(d). This shift is very likely due to the changes in refractive index of the semiconductor materials upon cooling. The combination of these boundary conditions essentially leaves the local-field parameter L as the only truly free parameter. It is expected to be similar for all SRR arrays, regardless of their resonance wavelengths.

In more detail, we compute the differential transmittance by taking the difference between the transmittance of the pumped case (assuming $f = 1$ occupation of the upper level) and the unpumped case (*i.e.*, $f = 0$) and normalize the result with respect to the unpumped transmittance. Using the Maxwell-Garnett approximation described in [14], the 30-nm thin layer of SRR and the 12.7-nm thin single QW are treated as a single effective layer with a thickness of 42.7 nm on top of a dielectric halfspace, the InP substrate. The InP refractive index is taken as $n = 3.1$ (independent of wavelength). In principle, the spectra obtained along these lines should finally be convoluted with the about 20-nm broad OPO probe spectrum. However, for the present conditions, the resulting effects turn out to be unimportant (not shown). Thus, we avoid this process step here. For all samples "A" to "I", the following model parameters (same nomenclature as in [14]) are fixed: $\Omega_{2LS} = 2\pi \times 205$ THz, $\gamma_{2LS} = 50$ THz, $d_{2LS} = 6.5 \times 10^{-29}$ Cm, $N_{2LS} = 2.1 \times 10^{24}$ m^{-3}, $\gamma_{pl} = 90$ THz, $d_{pl} = 4.2 \times 10^{-26}$ Cm, and $N_{pl} = 5.3 \times 10^{20}$ m^{-3}. The plasmonic resonance frequencies Ω_{pl} and the local-field parameters L for all samples shown in this paper are listed in Table 1.

Corresponding results are also shown in Fig. 4, allowing for direct comparison with experiment. Obviously, the general agreement between experiment and toy model is excellent considering the complexity of the overall behavior. In particular, we again find that negative differential transmittance signals $\Delta T/T$ are the rule rather than the exception. These negative signals are mainly due to reduction of the damping of the SRR transmittance minimum (see discussion in Section 1). Furthermore, in agreement with experiment, we find that the magnitude of the $\Delta T/T$ signals is substantially larger for the case of QW and SRR compared to the case of the QW alone. Let us emphasize, as already discussed in Section 1, that without any coupling between SRR and QW, *i.e.*, for local-field parameter $L = 0$, the $\Delta T/T$ signals for the case of QW and SRR and the case of QW alone would be just identical (not shown) – in striking disagreement with the experimental facts. This once again emphasizes that our results imply a considerably strong local-field coupling between the SRR and the QW gain – which is at the heart of our aim of reducing the metamaterial's losses. (The fitted local field coupling parameter L for sample "I" is an anomaly. The fit procedure for this very off-resonant sample turns out to be ambiguous.)

Table 1. Model parameters Ω_{pl} and L that are individually adjusted for samples "A" to "I" (compare Fig. 4).

sample	Ω_{pl}	L
A	$2\pi \times 241$ THz	1.8×10^{10} F/m
B	$2\pi \times 205$ THz	1.7×10^{10} F/m
C	$2\pi \times 203$ THz	1.8×10^{10} F/m
D	$2\pi \times 195$ THz	2.1×10^{10} F/m
E	$2\pi \times 193$ THz	1.8×10^{10} F/m
F	$2\pi \times 190$ THz	2.1×10^{10} F/m
G	$2\pi \times 187$ THz	2.2×10^{10} F/m
H	$2\pi \times 183$ THz	2.1×10^{10} F/m
I	$2\pi \times 175$ THz	0.1×10^{10} F/m

Let us note in passing that the simple toy model [14] cannot describe the Purcell effect, *i.e.*, the near-field non-radiative energy transfer from the QW to the SRR. In the limit of weak probe field and in absence of any spontaneous contributions, the upper-state two-level-system occupation f relaxes exponentially with rate Γ_{2LS} from $f = 1$ to $f = 0$ [see Eq. (5) in Ref.14]. Subsequently, for the present parameters, all $\Delta T/T$ signals with and without SRR show the same exponential decay (in sharp contrast to, *e.g.*, the experimental data in Fig. 2).

Finally, it is interesting to ask on the basis of the toy model: How far are we away from the original aim of completely compensating metamaterial losses? Let us consider the best case, *i.e.*, that the two-level system (2LS) resonance frequency Ω_{2LS} representing the QW and the plasmonic resonance (pl) frequency Ω_{pl} representing the SRR array are degenerate. Under this condition, a simple and transparent way to summarize the influence of the various parameters is to start from the loss = gain condition (lasing spasing condition) (Eq. (13) in [14]) for the two-level system upper-state occupation f, *i.e.*, from

$$f = \frac{1}{2}\left(1 + \frac{\gamma_{pl}\gamma_{2LS}}{V_{pl}V_{2LS}}\right) =: \frac{1}{2}\left(1 + \frac{\gamma^2}{V^2}\right) \in [0,1]. \qquad (1)$$

Here, γ_{2LS} and γ_{pl} are the damping frequencies of the two-level system and the plasmonic resonance. The quantities V_{2LS} and V_{pl} are the respective effective coupling frequencies given by (Eq. (9) in [14])

$$V_{2LS} = \hbar^{-1} d_{2LS} L N_{pl} d_{pl},$$

$$V_{pl} = \hbar^{-1} d_{pl} L N_{2LS} d_{2LS}. \qquad (2)$$

The condition (1) is graphically illustrated in Fig. 5. In the gray triangle, the loss = gain condition can *not* be fulfilled because f has a mathematical solution outside the interval [0,1]. In other words, the available gain is simply not sufficient to compensate for the losses. In the white triangle, the loss = gain condition can be fulfilled, even under continuous-wave self-consistent conditions. The red dot corresponds to the parameters that we have used to fit to the experimental data in Fig. 2.

To move the red dot into the white triangle, one could, *e.g.*, increase the QW dipole moment d_{2LS} by a factor of three to four ("more gain"). Alternatively, one could increase the local field coupling parameter L by the same factor ("more effective metamaterials at fixed QW gain"), or reduce the SRR damping ("less loss"), or reduce the QW damping ("more gain") by the same factor. On the basis of the experimental results of this paper, these parameter improvements are not quite impossible, but are not simple to reach either. Other material systems may have to be chosen.

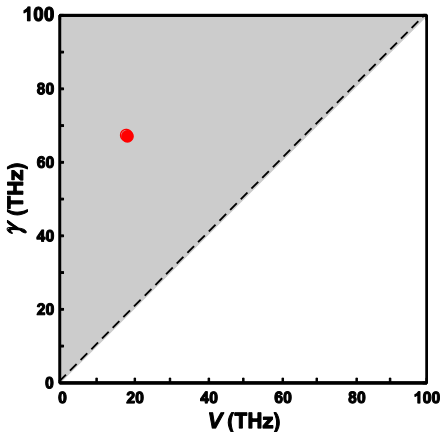

Fig. 5. Illustration of the loss = gain condition for the case that the quantum-well and the split-ring-resonator resonances are degenerate [see Eq. (1)]. Complete loss compensation is possible within the white triangle, but is not possible in the gray triangle. The two triangles are separated by the straight line with $\gamma = V$ [see Eq. (1)]. The red dot inside the gray triangle corresponds to the experimental conditions of sample "D" and is obtained from exactly the same model parameters that we have used to fit to these experimental results (compare Fig. 4).

5. Conclusions

We have presented experiments aiming at compensating the metal losses of arrays of SRR by coupling to an optically pumped InGaAs single quantum well *via* the local (or evanescent) electromagnetic fields of the SRR. We observe differential transmittance signals from the coupled system that are a factor of four to five larger than for the bare quantum well. Furthermore, we observe a more rapid temporal decay of the differential transmittance signal for the coupled system compared to the bare quantum well. Both effects indicate substantial local-field-enhancement effects, which increase the effective metamaterial gain beyond the bare quantum-well gain, leading to a significant reduction of the metamaterial's losses. This interpretation is also confirmed by comparison of the experimental data with a recently introduced analytical toy model. However, despite of the fact that we have employed very intense pulsed optical pumping and that we have cooled the samples to helium temperatures and that we have optimized the semiconductor-wafer design, the magnitude of the effect is too small to obtain complete metamaterial-loss compensation in our experiments.

Acknowledgements

We acknowledge support by the Deutsche Forschungsgemeinschaft (DFG) and the State of Baden-Württemberg through the DFG-Center for Functional Nanostructures (CFN) within subproject A1.5. The project PHOME acknowledges the financial support of the Future and Emerging Technologies (FET) programme within the Seventh Framework Programme for Research of the European Commission, under FET-Open grant number 213390. The project METAMAT is supported by the Bundesministerium für Bildung und Forschung (BMBF). The PhD education of N.M. and M.R. is embedded in the Karlsruhe School of Optics & Photonics (KSOP). Work at Ames Lab was supported by Dept. of Energy (Basic Energy Sciences), contract No. DE-AC02-07CH11358. The Tucson group thanks AFOSR, NSF AMOP, and NSF ERC CIAN for support. H.M.G. and J.H. thank the Alexander von Humboldt Foundation for a Renewed Research Stay and Junior Scientist Award, respectively.